13th International Symposium on Particle Image Velocimetry – ISPIV 2019
Munich, Germany, July 22-24, 2019

Flow Characteristics of a Plane Jet Perturbed by Rectangular Tabs at a Slot Nozzle Exit

Yudai Mikami[1], Takahiro Kiwata[2]*, Kohei Noguchi[1] and Kuniaki Toyoda[3]

[1] Kanazawa University, Graduate School of Natural Science and Technology, Kanazawa, Japan

[2] Kanazawa University, School of Mechanical Engineering, Kanazawa, Japan

[3] Hokkaido University of Science, Sapporo, Japan

* kiwata@se.kanazawa-u.ac.jp

Abstract

The effects of different rectangular tabs at the exit of a slot nozzle on the flow characteristics and vortical structures of a plane jet at relatively low Reynolds numbers were investigated to achieve passive control of the spread of the jet. Flow visualization and velocity measurements were performed using particle image velocimetry. In addition, 3-dimensional numerical simulation was performed using ANSYS Fluent to investigate the vorticity and the vortical structures of the plane jets. It was observed that the spanwise vortical structure of a plane jet disappeared completely when rectangular tabs were attached at the nozzle exit. Good agreement was found between the experiments and numerical simulations when large-eddy simulation was employed in the near-field region. We found that the nozzle exit with the smallest rectangular tabs had the smallest plane jet spread downstream, and the jet's centerline velocity at $2{,}000 \le Re \le 10^4$ was larger than that of jets without tabs.

1 Introduction

Plane jets are encountered in many engineering applications and manufacturing processes, such as cooling, drying, and removal devices. Plane jets are also used to create air doors, invisible air curtains that separate two open spaces. For air doors especially, plane jets with a small spread are desirable. Because the spread is influenced by the vortical structures in plane jets, a better understanding of how to control the occurrence and development of vortices in free shear layers is needed.

The flow characteristics of plane jets have been studied by several researchers. Deo et al. (2007, 2008) investigated the effect of the geometric profile of a slot nozzle on the statistical properties of a plane jet issuing from a long rectangular slot nozzle with a large aspect ratio of 60. In particular, they measured the effect of Reynolds number (*Re*) for *Re* values in the range of 1.5×10^3 to 1.65×10^4. They found that the effect of Reynolds number on both the mean and turbulent fields is substantial for $Re < 10^4$ but becomes weaker as the Reynolds number increases. Gori et al. (2014) presented flow visualizations and measurements for an air jet issuing from a rectangular nozzle with an aspect ratio of about 6.2 and $Re = 2.0\times10^3$ to 3.53×10^4, and showed that the effect of Reynolds number on the instant flow evolution and undisturbed flow region decreases as the Reynolds number increases.

A number of researchers have tried to passively control the flow development of plane jets. For example, jets can be passively controlled without an external energy supply by perturbing the flow with tabs and deflectors at the nozzle exit. Sakai et al. (2016) and Kiwata et al. (2018) investigated the characteristics of a plane jet with tabs at the slot nozzle exit using experiments and numerical analysis at a low Reynolds number (Re = 2,000). They found that tabs produce shear layers and streamwise vortices that reduce the plane jet spread. Further, the spread of a plane jet from a nozzle with square tabs was smaller than that from a nozzle with triangular tabs. Finally, they found that the slant angle and installation arrangement of tabs influence the length of the region without turbulent flow, that is, the potential core length of the plane jet.

The purpose of this study was to clarify the effects of different rectangular exit tab shapes on the flow characteristics and vortical structures of plane jets at low Reynolds numbers ($Re \leq 10^4$). This paper describes the velocity, turbulence intensity, vorticity distributions, and influence of Reynolds number obtained experimentally using particle image velocimetry (PIV), and also obtained numerically by ANSYS Fluent, a commercially available computational fluid dynamics (CFD) application.

2 Experimental apparatus and method

2.1 Experimental setup

A schematic diagram of the experimental apparatus is shown in Fig. 1. A centrifugal fan was used to supply an airflow to a settling chamber with porous plates. The chamber was constructed out of acrylic plastic, and its height, length and width (span) were 700, 645, and 400 mm, respectively. The airflow converged at a planar slot with round corners. The streamwise length of the planar nozzle was 30 mm, and its span was B = 300 mm.

The present study focuses on the effect of different rectangular tabs at the nozzle exit. The arrangement of the rectangular tabs at the nozzle exit and their shapes and sizes are shown in Figs. 2 and 3. Four different shapes were used; rectangular-B and D tabs had the same shape and size but different spacing. The height of the plane nozzle between the bottom of the tabs varied from H = 6.4 to 7.8 mm so that the area of the nozzle exit was constant for each arrangement. As a result, the equivalent nozzle height was set as H_e = 5 mm to match the exit area of the planar nozzle without tabs (1,500 mm^2). The x, y, and z directions corresponded to the nozzle streamwise, height, and span directions, respectively.

2.2 Experimental method

The 2-dimensional flow fields of the plane jets were measured using PIV. Continuous image pairs were acquired at a frame frequency of 10 Hz and pixel resolution of 2,048×2,048 with a CCD camera (DANTEC FlowSense EO 4M) and processed by the commercially available DANTEC Dynamic Studio Ver. 5.1 software suite. A double-pulse Nd:YAG laser (Dual Power 200-15, 200 mJ) was used to produce light sheets in the x-y and y-z planes. The size of the interrogation window was 120 and 120 mm in the x and y directions, respectively. A fog generator (SAFEX Fog Generator) was used to produce an oil mist to provide tracer particles with mean diameters of approximately 1 μm. The particle fluid density was 1,030 kg/m^3. The PIV system was also employed for the visualization of

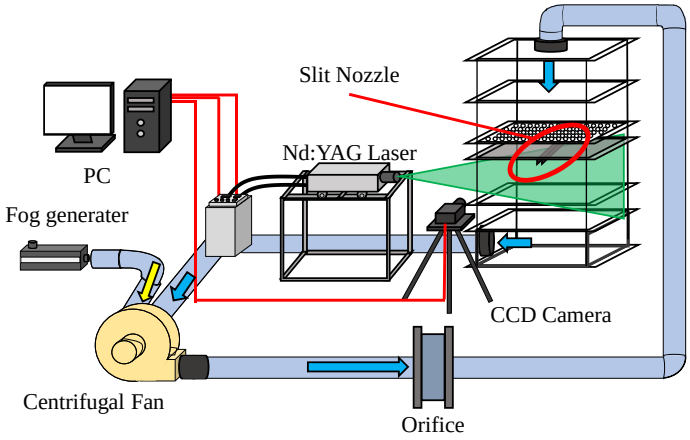

Figure 1: Schematic diagram of experimental apparatus

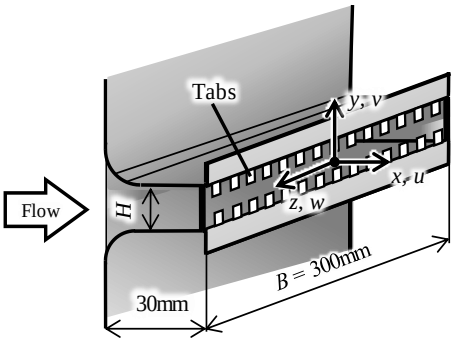

Figure 2: Schematic diagram of slot nozzle with tabs

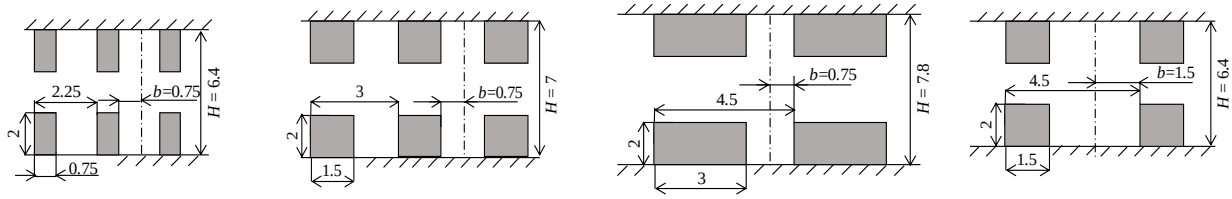

(a) Rectangular-A tabs (b) Rectangular-B tabs (c) Rectangular-C tabs (d) Rectangular-D tabs

Figure 3: Sizes, shapes, and spacing of rectangular tabs

vortical structures in the plane jet. The spatial density of particles in the flow visualization working fluid was much larger than that used for the PIV system velocity measurements.

The mean velocity at the nozzle exit in the potential core was varied over the range 3 to 30 m/s for each nozzle configuration. The Reynolds number, which was based on the equivalent nozzle height H_e and the nozzle exit mean velocity U_0, was varied from 1,000 to 10^4 to investigate its influence on the jet flow fields.

3 Numerical methodology

3.1 Governing equation and numerical procedure

The flow field was assumed to be unsteady, viscous, and incompressible. To provide comparisons with experimental results, numerical simulations were performed using ANSYS Fluent 15.0 based on the finite-volume method for the initial condition of laminar steady flow, and large-eddy simulation (LES) for the unsteady flow. The governing equations for LES were filtered Navier-Stokes and continuity equations. The dynamic Smagorinsky-Lilly model was used at the sub-grid scale. The convection terms of the governing equation were discretized by the bounded central differencing scheme. Second-order central differencing was used for the diffusion term, while the second-order implicit scheme was used for the time progression. The pressure implicit with the splitting-of-operators (PISO) method was used as the calculation algorithm for the pressure-velocity coupling.

3.2 Computational mesh and boundary conditions

Figure 4 shows the computational domain, mesh, and boundary conditions. To improve the turbulence sensitivity (and thus accuracy) in the vicinity of walls and the nozzle, the computational meshes used for the LES were set finer than those for the laminar simulations. The streamwise and transverse lengths of the computational domain were 170 mm (= $34H_e$) and 300 mm (= $60H_e$), respectively. The parallel channel nozzle length was 30 mm (= $6H_e$), and the nozzle span was the same as 10 pitch lengths of the rectangular-A and B tabs and 5 pitch lengths of the rectangular-C and D tabs. The computational mesh was created with an unequally spaced structure. The number of grid points for LES was about 3.0×10^6. The spanwise boundary of the computational domain was set as a periodic boundary condition. The top and bottom boundaries of the computational domain satisfied the slip condition. A pressure outlet condition of $p = 0$ was specified at the downstream boundary of the domain. The velocity at the upper and lower inlet surfaces, which were parallel with the nozzle inlet surface, was adjusted to $0.03U_0$ to maintain a weak straight flow aimed toward the entrainment flow outlet. In the case of LES, a turbulence intensity of 3% was employed on the nozzle inlet surface. The numerical result obtained by the laminar model was used as initial conditions for LES.

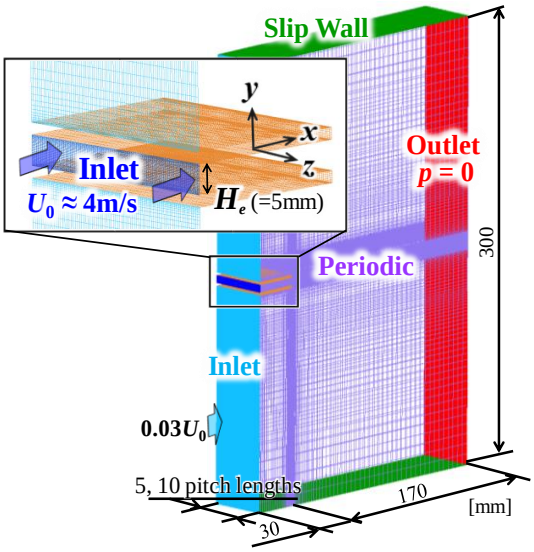

Figure 4: Computational domain showing mesh and boundary conditions

4 Results and discussion

4.1 Influences of Reynolds number and tab shape

Figure 5 shows the variations of the centerline mean x-axial velocity $\bar{u}_c/U_0$ of a plane jet with rectangular-B tabs at different Reynolds numbers. The potential core length x_p is defined to be the axial location at $\bar{u}_c \approx 0.98U_0$. The non-dimensional potential core length was $x_p/H_e \approx 11$ at low Reynolds numbers of $1{,}000 \le Re \le 2{,}000$. At $3{,}000 \le Re \le 10^4$, the non-dimensional potential core length was $x_p/H_e \approx 5$. After the potential core collapsed, the centerline mean velocity decreased at $\bar{u}_c/U_0 \approx x^{-1}$ at low Reynolds numbers of $1{,}000 \le Re \le 2{,}000$ and $\bar{u}_c/U_0 \approx x^{-2/3}$ at $4{,}000 \le Re \le 10^4$.

Figure 6 shows the variations of potential core length with Reynolds numbers for all tabbed plane jets. The non-dimensional potential core length of a plane jet was the longest at $Re \ge 2{,}000$ with rectangular-A tabs. The non-dimensional potential core length of a plane jet with rectangular tabs at $Re \ge 2{,}000$ generally decreased as the Reynolds number increased. Thus, the flow characteristics of a plane jet from a nozzle with rectangular tabs in the range of $2{,}000 \le Re \le 4{,}000$ seems to transition from laminar to turbulent flow.

Figure 7 shows the mean centerline velocity $\bar{u}_c/U_0$ and the mean x-axial velocity fluctuation $u_c'_{rms}/U_0$ of a plane jet at Re = 2,000 and 4,000. The mean centerline velocities obtained by CFD at Re = 2,000 are also shown in Fig. 7(a). The centerline mean velocity of the plane jet from a nozzle without tabs was smaller than that from a nozzle with tabs. In other words, the presence of rectangular tabs lengthens the potential core of a plane jet. After collapse of the potential core, the centerline mean velocity from a nozzle with rectangular tabs decreases at $\bar{u}_c/U_0 \approx x^{-1}$ and Re = 2,000. The LES results and the experimental results are in good agreement. After the disappearance of the potential core at $x/He > 9$, the velocity fluctuation of the plane jet from nozzles with tabs increases gradually. At Re = 4,000, after the potential core collapse, the centerline mean velocity from the nozzle with rectangular-A tabs decreases at $\bar{u}_c/U_0 \approx x^{-2/3}$, and the centerline mean velocity from nozzles without tabs decreases at $\bar{u}_c/U_0 \approx x^{-1/2}$, as is the case for a 2-dimensional turbulent plane jet. Thus, the ratio of decreasing centerline mean velocity depends on the shape of the tab and the Reynolds number.

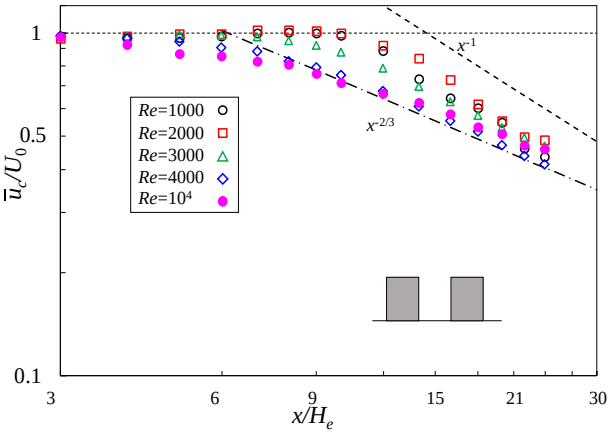

Figure 5: Variation of mean jet centerline velocity of a plane jet with rectangular-B tabs for different Reynolds numbers

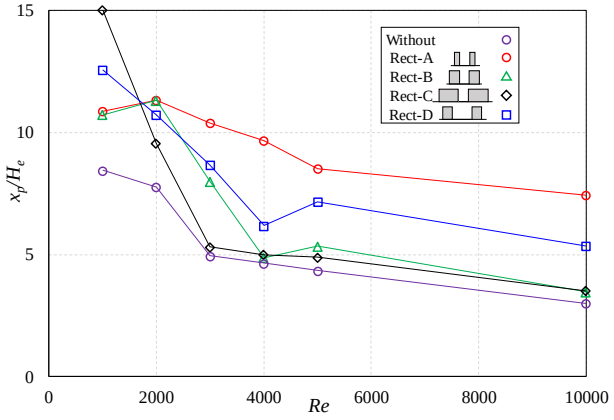

Figure 6: Variation of potential core length with different Reynolds numbers

The streamwise variation of the half width of a plane jet from nozzles without and with tabs is shown in Fig. 8. After the potential core collapses, the spread of the plane jet increases. At Re = 2,000, the half width of a plane jet with rectangular-B tabs is lower than that with the other tabs. At Re = 4,000, the half width of a plane jet with rectangular-A tabs is lower than the other tabs. For a plane jet with rectangular-C tabs, the half width is larger than that of the other tabs at Re = 2,000 and 4,000.

4.2 Flow visualization of vortices in plane jets

Figure 9 shows the instantaneous flow patterns of a plane jet from nozzles without and with rectangular tabs for Re = 2,000 at the x-y cross section (z = 0). The flow visualization of the plane jet without tabs reveals that the potential core length is $x_p/H_e \approx 8$, and periodic spanwise vortical structures are apparent in the free shear layers after the potential core collapses. The length of the potential core region near the jet axis in a plane jet extending from a nozzle with rectangular tabs is greater than that from a nozzle without tabs. The spanwise vorticities appear farther downstream and become smaller.

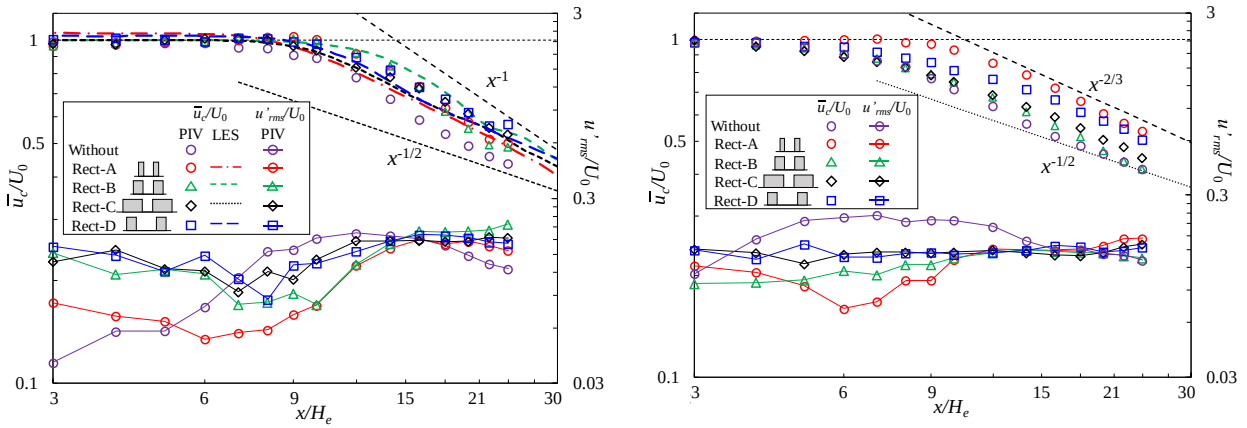

(a) *Re* = 2,000 (b) *Re* = 4,000

Figure 7: Mean velocity $\bar{u}_c/U_0$ and the mean x-axial velocity fluctuation $u_c'_{rms}/U_0$ on the centerline of jets

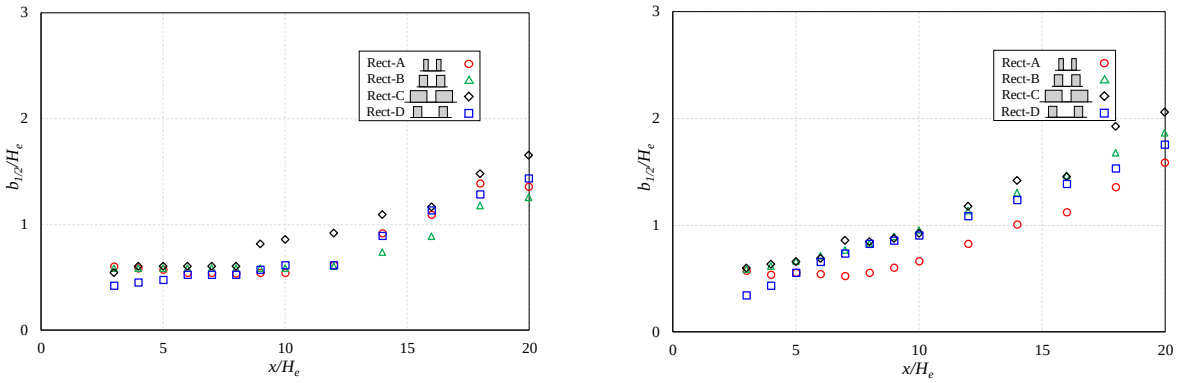

(a) *Re* = 2,000 (b) *Re* = 4,000

Figure 8: Streamwise variation of half width of plane jets

Figure 10 shows the instantaneous flow patterns of a plane jet from a nozzle without and with rectangular tabs for *Re* = 4,000 at the x-y cross section (z = 0). The presence of large spanwise vortical structures is apparent in the plane jet without tabs in the near field from $x/H_e \approx 4$. Consequently, the potential core length decreases with respect to that at *Re* = 2,000. When tabs are present in a slot nozzle, small-scale vortices appear in the resulting plane jet. The potential core length also decreases with respect to that at *Re* = 2,000.

Figure 11 shows the instantaneous flow patterns of plane jets from nozzles without and with rectangular tabs at the y-z cross section for *Re* = 2,000 and 4,000 (x/H_e = 4). No streamwise vortical structure is found in the shear layers of a plane jet from a nozzle without tabs. With rectangular tabs at *Re* = 2,000, a streamwise vortical structure similar to a cirriform vortex is formed in the jet. The size of streamwise vortices formed by a nozzle with rectangular-A tabs is smaller than that formed by the other tabs. For *Re* = 4,000, the streamwise vortices of the plane jet with rectangular-A tabs can be found at x/H_e = 4. Thus, the streamwise vortices produced downstream of a nozzle with tabs can prevent the attenuation of the centerline mean velocity and the spread of the plane jet.

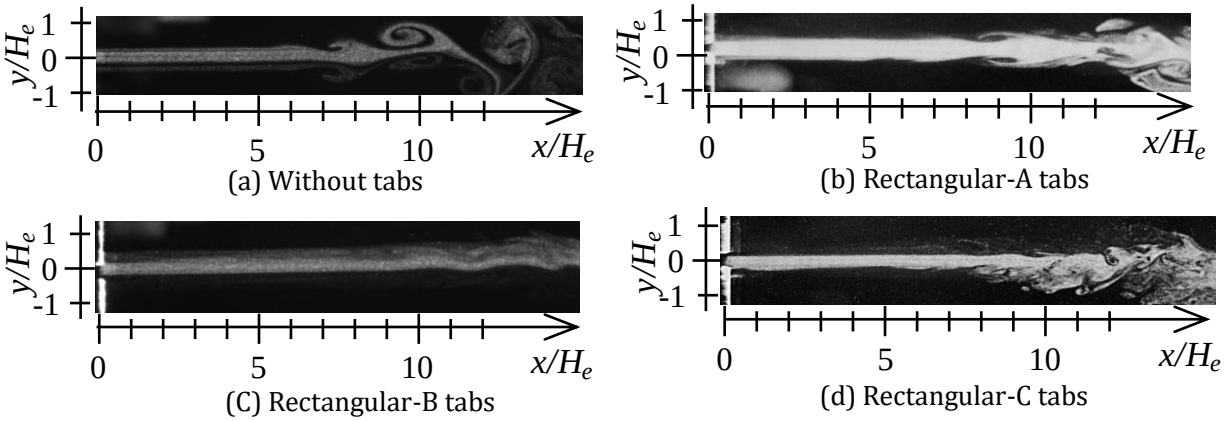

(a) Without tabs (b) Rectangular-A tabs

(C) Rectangular-B tabs (d) Rectangular-C tabs

Figure 9: Instantaneous flow pattern of various plane jets at the *x-y* cross section for *Re* = 2,000 (*z* = 0)

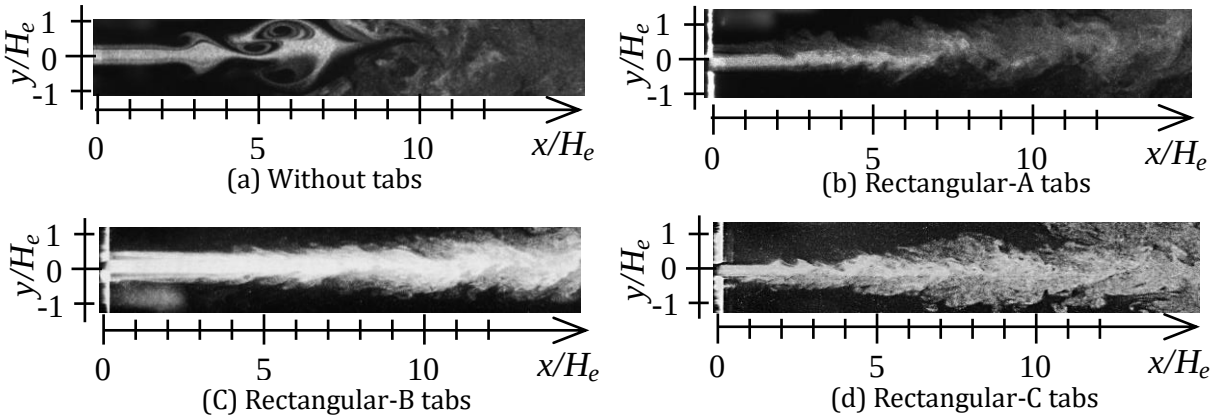

(a) Without tabs (b) Rectangular-A tabs

(C) Rectangular-B tabs (d) Rectangular-C tabs

Figure 10: Instantaneous flow patterns of plane jets at the *x-y* cross section for *Re* = 4,000 (*z* = 0)

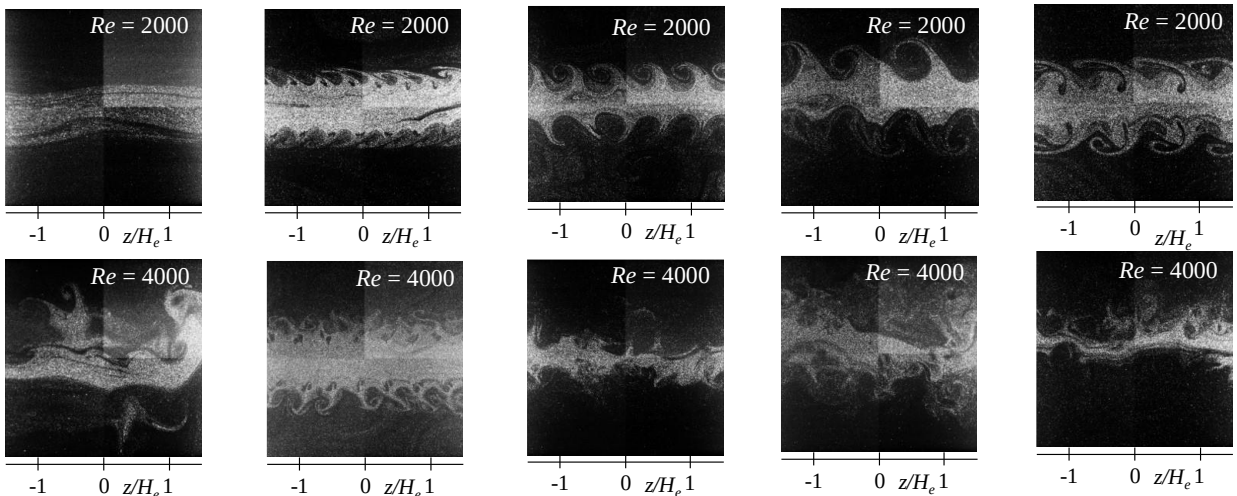

(a) Without tabs (b) Rectangular-A tabs (c) Rectangular-B tabs (d) Rectangular-C tabs (e) Rectangular-D tabs

Figure 11: Instantaneous flow patterns of plane jets at the *y-z* cross section for *Re* = 2,000 and 4,000 (x/H_e = 4).

4.3 Prediction of the flow structure by LES

Figure 12 shows the second invariant LES iso-surfaces of the velocity gradient tensor Q for plane jets from nozzles with rectangular tabs. It can be seen that all of plane jets from nozzles with rectangular tabs have a streamwise vortical structure. For plane jets formed with rectangular-A and B tabs, the spaces between the streamwise vortices are smaller than those formed with rectangular-C and D tabs, and the streamwise vortical structure persists downstream. For plane jets formed with rectangular-C tabs, the spaces between the streamwise vortices are larger than those formed with rectangular-A and B tabs, and streamwise vortices merge with their neighbors. Consequently, the streamwise vortical structure collapses downstream. These results reveal that the streamwise vortices in the shear layers for the plane jet from the nozzle with rectangular-A tabs contributes to formation of a flow state with small disturbances.

Figure 13 shows the contours of the x-axial vorticity ξ_x of plane jets from nozzles with rectangular tabs obtained via LES. For a plane jet with rectangular-A tabs, at x/H_e = 2, positive and negative pairs of streamwise vorticities are generated near the top and bottom of the tabs. In the downstream region of x/H_e = 4, the streamwise vorticities at the bottom of tabs becomes weaker than the top vorticities. For plane jets with rectangular-B tabs, positive and negative streamwise vorticities are generated at the tab corners at x/H_e = 2, and the vorticity becomes weak at x/H_e = 4. For plane jets formed with

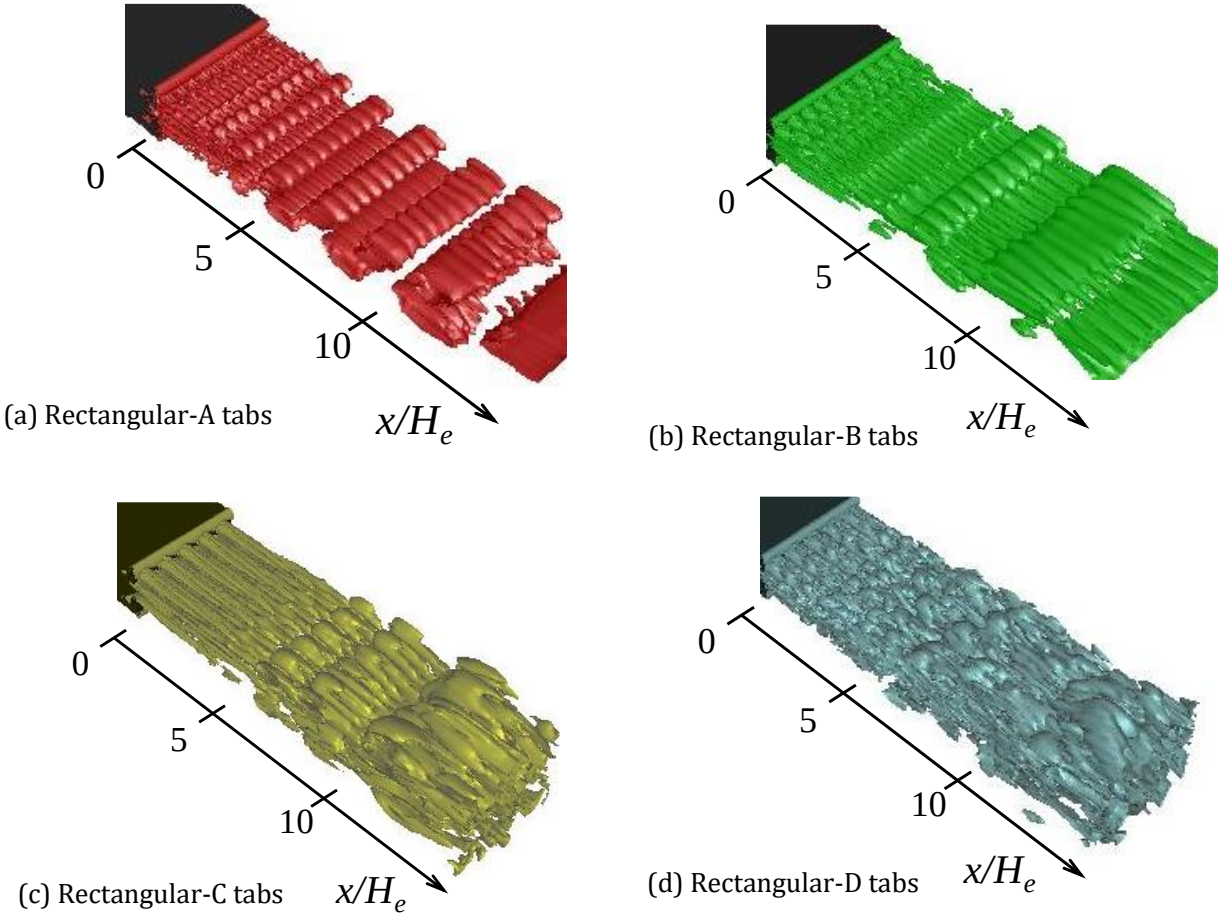

(a) Rectangular-A tabs (b) Rectangular-B tabs

(c) Rectangular-C tabs (d) Rectangular-D tabs

Figure 12: Instantaneous second invariant iso-surface of the velocity gradient tensor Q of plane jets (Re = 2,000)

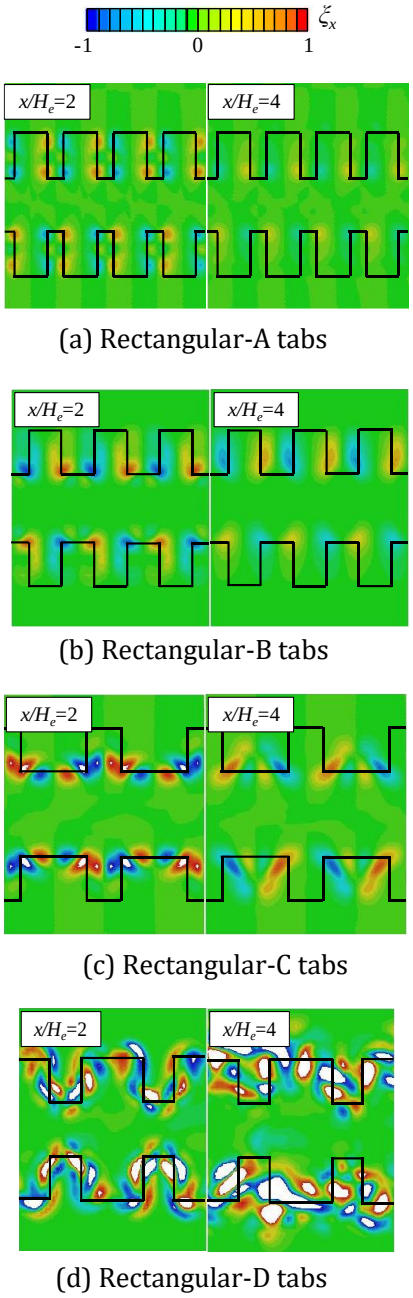

(a) Rectangular-A tabs

(b) Rectangular-B tabs

(c) Rectangular-C tabs

(d) Rectangular-D tabs

Figure 13: Instantaneous contours of x-axial vorticity ξ_x (Re = 2000, LES)

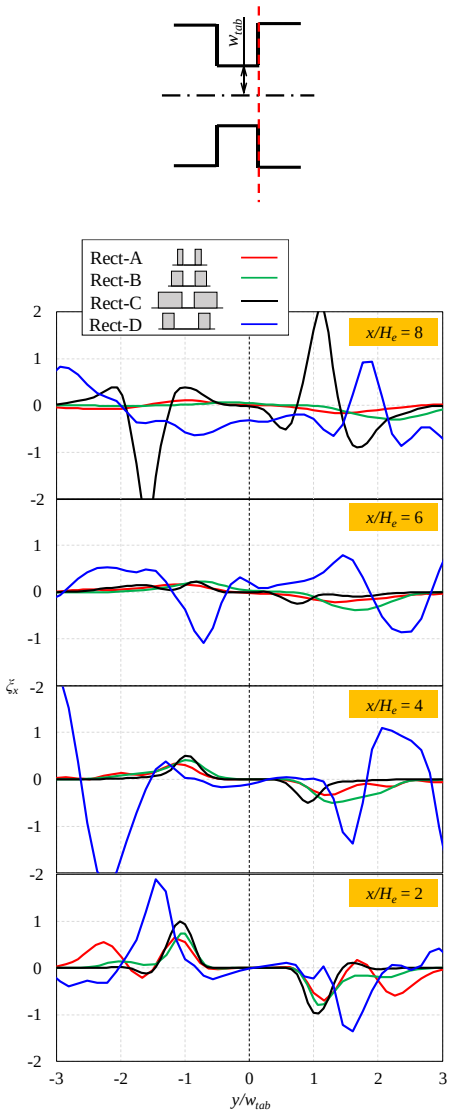

Figure 14: Profiles of instantaneous x-axial vorticity ξ_x (Re = 2,000, LES)

rectangular-C tabs, positive and negative pairs of streamwise vorticities are generated at the center and corners of tabs at x/H_e = 2, and the vortices extend obliquely. For plane jets formed with rectangular-D tabs, the positive and negative streamwise vorticities with larger magnitude are generated at the corners and bottom of tabs.

Figure 14 shows the profiles of x-axial vorticity ξ_x at the vertical cross-section of the side surface of tabs obtained via LES. The distance from the centerline of the nozzle to the top of the tab is defined as w_{tab}. The position of the top of tab is y/w_{tab} = ±1. For plane jets from nozzles with rectangular-A and B tabs, the peak value of x-axial vorticity ξ_x is not larger than that from nozzles with the other tabs,

and it decreases with increasing x-direction distance. However, for plane jets from nozzles with rectangular-C and D tabs, the peak value of x-axial vorticity ξ_x becomes larger at $x/H_e = 8$ than it does with the rectangular-A and B tabs. Incremental increases of mixing with the ambient fluid and the potential core length are also related to the growth of streamwise vortices.

5 Conclusions

The flow characteristics and vortical structures of a plane jet perturbed by tabs at the nozzle exit were investigated using experiments and numerical simulations at the low Reynolds numbers of $1{,}000 \leq Re \leq 10^4$. The results lead to the following conclusions:

(1) The flow characteristics of a plane jet from nozzles with rectangular tabs in the range of $2{,}000 \leq Re \leq 4{,}000$ transition from laminar to turbulent flow.

(2) The vorticity of streamwise vortices depends on the shape of the tab, and it increases with an increase in the width of tab.

(3) For a plane jet from a nozzle with rectangular-A tabs, the potential core length is longer and the jet spread is smaller than that from nozzles with larger tabs because streamwise vortices with low vorticity are maintained further downstream.

References

Deo R. C., Mi J., and Nathan G. J. (2007) The Influence of Nozzle-Exit Geometric Profile on Statistical Properties of a Turbulent Plane Jet. *Experimental Thermal and Fluid Science*, 32: 545-559.

Deo R. C., Mi J., and Nathan G. J. (2008) The influence of Reynolds number on a plane jet. *Physics of Fluids*, 20: 075108-1- 075108-16.

Gori F., Petracci I., and Angelino M. (2014) Influence of the Reynolds number on the instant flow evolution of a turbulent rectangular free jet of air. *International Journal of Heat and Fluid Flow*, 50: 386-401.

Kiwata T., Mikami Y., Kono T., and Toyoda, K. (2018) Effects of slant angle and installation arrangement of nozzle exit tabs on flow characteristics of a plane jet. *Proceedings of 18th International Symposium on Flow Visualization Zurich, Switzerland,* A-0964-0002-00209: 1-9.

Sakai M., Kiwata T., Awa T., Teramoto H., Kono T., and Toyoda K. (2016) Experimental and Numerical Investigations of Tab Geometry Effects on Flow Characteristics of a Plane Jet. *Proceedings of the 2016 Asia-Pacific International Symposium on Aerospace Technology, Toyama,* F9-2: 1-8.